Crystallization Kinetics and Polymorphism in Aromatic Polyketones (PEKEKK) with Different Molecular Weight

D. R. Rueda, M. C. García Gutiérrez, F. Ania, M. G. Zolotukhin,† and F. J. Baltá Calleja*

Instituto de Estructura de la Materia, CSIC, Serrano 119, Madrid 28006, Spain

Received March 20, 1998; Revised Manuscript Received August 26, 1998

ABSTRACT: Simultaneous wide and small X-ray scattering (WAXS and SAXS) real time experiments using synchrotron radiation were performed to investigate poly-aryl(ether ketone ether ketone ketone) (PEKEKK) samples with different molecular weights obtained by precipitation polycondensation. Isothermal melt crystallization experiments, using two crystallization temperatures, T_c (differing by 10 °C) for each polymer grade were carried out. The phase transition temperature from polymorphic form II to form I was investigated in the samples as obtained. The variation of the index of crystallinity during heating was shown to depend on molecular weight. The index of crystallinity and X-ray long period values of the isothermal melt-crystallized samples observed at T_c and then at room temperature depend on the T_c values. For the lowest viscosity sample the microstructure is also molecular weight dependent. Avrami analysis of the 110(I) reflection leads to the conclusion that a similar crystallization mechanism takes place for the samples investigated.

Introduction

Aromatic poly(ether ketone)s as high-performance thermoplastic materials have received special attention in the past decade.[1−3] These polymers show high thermostability and chemical resistance.[2,3] They can be considered as linear polymers of intermediate chain rigidity since polymer chains consist of bulk phenyl rings linked by oxygen and ketone groups. Samples with high viscosity values, i.e., high molecular weights, have been obtained by the precipitation polycondensation method[4,5] using very low monomer concentrations.[6]

It is known that the thermal properties (melting and glass transition temperatures) of aromatic polyketones are dependent on the ether/ketone ratio, which influences the lattice parameters of the orthorhombic unit cell. Chain packing is similar to that found for poly(phenylene oxide)[7] and PEEK.[8−10] For polyketones with carbonyl contents larger than 50% (PEKEKK and PEKK) Blundell and Newton[11] observed additional reflections in the X-ray patterns of oriented samples that revealed the presence of a new orthorhombic crystallographic form with *a* and *b* axes exchanged with each other.

Gardner et al. reported on the polymorphism of aromatic polyketones with different ether/ketone ratios[12,13] crystallized under different conditions and for polyketones containing isophthalic units.[12] In the case of polyketones crystallized from the melt the normal orthorhombic packing (PEEK-type or form I) is always observed for all polyketones independently of their carbonyl content. On the contrary, samples prepared by cold crystallization and solvent-induced crystallization, with a carbonyl content larger than 50% (PEKEKK, PEKK) showed exclusively the second crystallographic form mentioned above. In this paper we will refer to these crystallographic forms as forms I and II following Gardner's notation.

As far as isothermal crystallization is concerned, the influence of molecular weight on the crystallization kinetics of semirigid materials has attracted attention.[14−17] For both, cold and melt isothermal crystallization, the half-crystallization times $t_{1/2}$ strongly depend on the T_c values as well as on the molecular weight of the samples.[16] Thus, because reasonable experimentation times have to be used, it becomes an important task to determine the convenient T_c values for each sample. That is also so because comparison of crystallization kinetics parameters from different samples demands working under similar undercooling conditions. It is also known that the microstructure of isothermally melt-crystallized polymers, as revealed by their long periodicity (L) value, shows increasing L values up to a given value of the molecular weight. Beyond this value, the long periodicity remains constant and independent of molecular weight.[18] For this upper range of molecular weights the L values would mainly depend on the thermal crystallization conditions. Thus, larger L values are obtained for the smaller supercoolings (higher T_c values).

In previous studies we have reported on the synthesis, NMR characterization, and evaluation of the isomeric chain defects[6] and on the morphology of PEKEKK particles obtained.[6,19] We have additionally investigated the thermal behavior and structure of PEKEKK samples with different molecular weights.[20] It was found that molecular weight affects the index of crystallinity and melting behavior of the as-obtained and melt-crystallized samples. It was also shown that the as-obtained samples preferentially show crystallographic form II. After short annealing treatments form II partially converts into the more stable form I, as revealed by X-ray diffractograms recorded at room temperature. Although polymorphism is evidenced by X-ray diffraction, the DSC thermograms of the thermally treated samples appear, on the contrary, to be so simple that any polymorphism could be disregarded.[20]

The use of both wide (WAXS) and small angle X-ray scattering (SAXS) experiments in real time allows one

† Permanent address: Institute of Organic Chemistry, Prospekt Oktyabraya, 69, 450054 Ufa-54, Russia.

10.1021/ma980440z CCC: $15.00
Published on Web 10/22/1998

Table 1. Inherent Viscosity, Molar Content of Defect Isomer Chains, and Melt Temperatures of the Samples as Obtained[20]

sample	η_{inh} (dL/g)	defect isomer chains molar content (%)	T_m (1st run) (°C)	T_m (2nd run) (°C)
P1	1.46	6.7	373.5	369.9
P2	1.85	5.0	376.6	353.3
P3	2.42	2.4	385.6	342.5

to simultaneously follow the structural changes at the molecular and supramolecular (microstructure) levels during thermal treatment. In particular, these combined techniques are of great value for the study of precrystallization phenomena in polymers.[21−23]

The aim of this work is 2-fold: (a) to investigate the polymorphic phase transition (phase II into phase I) during heating at 10 K/min of the as-obtained PEKEKK samples and (b) to compare the isothermal crystallization of the molten material at two different T_c values differing by 10 °C. For this purpose simultaneous WAXS and SAXS experiments in real time using synchrotron radiation were performed.

Experimental Part

Materials. The chemical repeat unit of poly-aryl(ether ketone ether ketone ketone) is

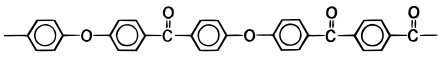

Three PEKEKK samples prepared by the precipitation polycondensation method, with different molecular weights (viscosities)[6] were investigated (Table 1). The molar content of the defect isomer and the melting temperature T_m measured from the first and a second consecutive DSC runs, previously reported,[20] are also included.

Techniques. For the X-ray investigation the as-obtained samples, in particle form, were sintered as disks.[20] The disks were wrapped with aluminum foil to improve thermal contact and to prevent loss of material when molten. A vacuum oven was used throughout the experiments. A similar temperature program for the three samples was applied: first, a fast heating to 200 °C for 2 min, followed by heating at a rate of 10 K/min up to 400, 405 and 410 °C, respectively, i.e., about 25 deg above the melting temperature of each sample (see Table 1). The sample was, then, maintained at this temperature for 10 min to improve the homogeneity of the molten state (erasing the particle structure). Finally, the sample was rapidly cooled (∼1 min) to the crystallization temperature, T_c. Two different T_c values separated by 10 °C were selected for each sample: P1(360 and 350 °C), P2 (343 and 333 °C), P3 (332 and 322 °C). Thus, our isothermal crystallization experiments are far from using a similar supercooling for the three samples; i.e., supercooling values increase from P1 to P3. Nevertheless, the choice of such T_c values was essentially aimed at guaranteeing a complete isothermal crystallization for all the three different molecular weight samples. It should be noted that the selected T_c values are related (10 and 20 °C below) to the T_m values measured from the second DSC run of the samples. (Table 1). Crystallization times above 3 h were chosen.

Synchrotron X-ray radiation, with wavelength $\lambda = 0.154$ nm, at the polymer beamline A2 of HASYLAB (DESY) was used. Two monodimensional wire detectors, with 512 channels each, simultaneously recorded wide and small angle X-ray scattering (WAXS and SAXS) patterns of the samples. The SAXS detector was located in front of the sample at a distance of about 2 m. The WAXS detector is placed at a certain angle from the X-ray beam showing a useful detection window between 9 and 33° (2θ). For calibration of the scattering angle in the WAXS and in the SAXS region a high-crystallinity PET sample and both a metal grid and a rat tail sample were respectively used. The resolution achieved for SAXS was less than 40 nm. A source of ^{55}Fe was employed to check the response of the detector to the radiation. Each X-ray scattering pattern was recorded for 0.5 min. The elapsed time between consecutive spectra was 1 ms during the heating cycle and the first part of the isothermal crystallization and 1 min for the rest of the isothermal crystallization.

X-ray scattering profiles were analyzed by means of PC software from HASYLAB. The Lorentz correction was applied to the SAXS intensity profiles (intensity is multiplied by s^2, where s is the scattering vector: $2 \sin \theta / \lambda$). A fit program was used to resolve both WAXS and SAXS intensity profiles into their single peak components. Particularly, WAXS diffractograms were fitted using Gaussian-type curves.

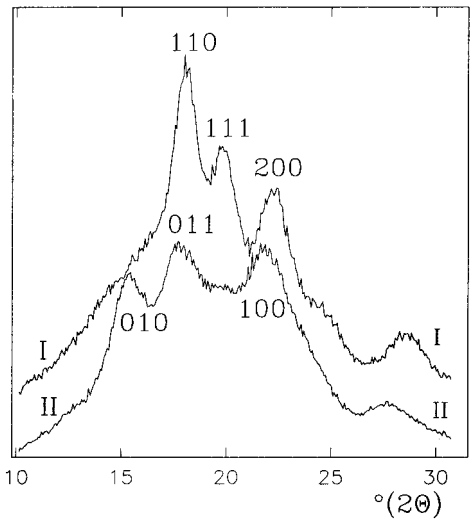

Figure 1. WAXS diffractograms recorded at room temperature, of aromatic polyketone sample P2 as obtained (phase II, bottom) and after melting and isothermal crystallization at 333 °C for about 3 h (phase I, top).

Results

Characterization of the Materials. Figure 1 shows the WAXS intensity curves observed at room temperature for the sample before thermal treatment (II) and after melting and recrystallization (I). Diffractogram I is representative of crystal modification I (melt-crystallized material) while diffractogram II can be mainly attributed to crystal modification II. The crystallographic indices for some representative reflections of each crystal phase are indicated. Note the close angular position of the reflections 011(II) and 100(II) in relation to 110(I) and 200(I). On the contrary, the 010(II) and 111(I) reflections appear well separated one from each other. Therefore, the two latter reflections are convenient for a rapid identification of each crystal modification.

Polymorphic Transition during Heating. Figure 2 illustrates the simultaneous change of the WAXS (top) and SAXS (bottom) intensity profiles for the P2 sample: (1) a change during a first heating at 10 K/min followed by a heating at $T = 405$ °C for 10 min and, finally, (2) the isothermal crystallization of the material at 333 °C.

The temperature program used (see Experimental Part) is schematically depicted along the time axis. Similar plots were recorded for the three investigated samples.

Let us follow the changes of the WAXS diffractogram (phase II) during heating of the sample (Figure 2 top).

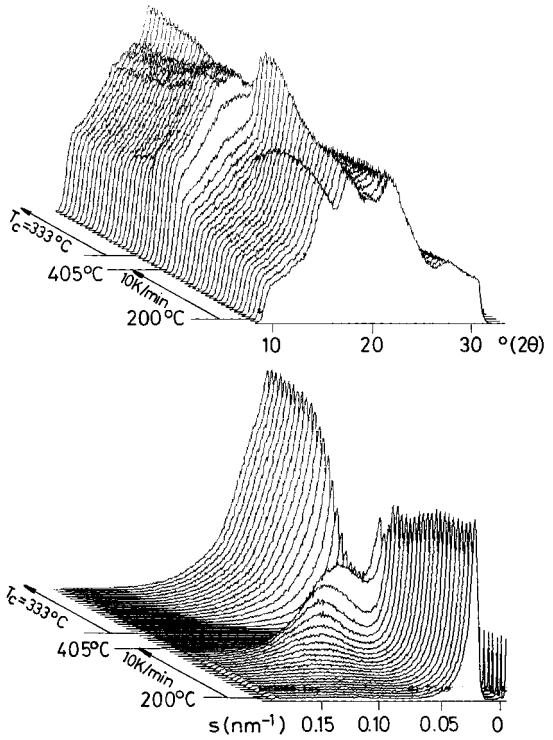

Figure 2. Change of WAXS (top) and SAXS (bottom) intensity profiles during heating of aromatic polyketone P2 as obtained above its melting temperature followed by isothermal crystallization.

The variation of the peak intensity of the three main reflections with increasing temperature is shown in Figure 3, for the P1 and P3 samples. As expected, there is a shift in temperature for the data of P3 as compared to P1 because of their different melting temperatures (Table 1). The differences observed in the initial relative intensity of the reflections for P1 and P3 are noteworthy. This can be attributed to the coexistence of phase II with a small amount of phase I in the case of P3.[19,20] Apart from that, a similar general behavior was observed for the three samples. The peak intensity of the 010(II) reflection gradually decreases for temperatures above 200 °C till its total disappearance at about 350 °C. On the other hand, the intensity of the 011(II) peak increases in the same temperature region and reaches a maximum at about 350 °C. This opposite behavior of the 010(II) and 011(II) reflections is due to the concurrent intensity development of the 110(I) reflection, which overlaps with the 011(II) peak. Similarly, the intensity of the reflection located at about 22.5°, (2θ), which may be indexed as 100(II) in the starting sample, decreases to a minimum at 290 °C and then increases, showing a maximum at 350 °C due to the progressive appearance of the 200(I) reflection. For P3, the intensity slightly decreases, then showing an increase with a maximum centered at about 360 °C. It is worth mentioning that the 111(I) reflection (Figure 1) becomes clearly resolved above 300 °C and shows also a maximum intensity at 360 °C. Therefore, it can be concluded that the total disappearance of the reflections of phase II corresponds with the maximum intensity observed for the reflections of phase I.

Concerning the lattice spacings, a similar variation was observed for the three investigated samples. Figure 4 illustrates the temperature dependence of the d_{011} and d_{100} spacings for the P3 sample. Besides the positive slope due to the thermal lattice expansion, a deviation

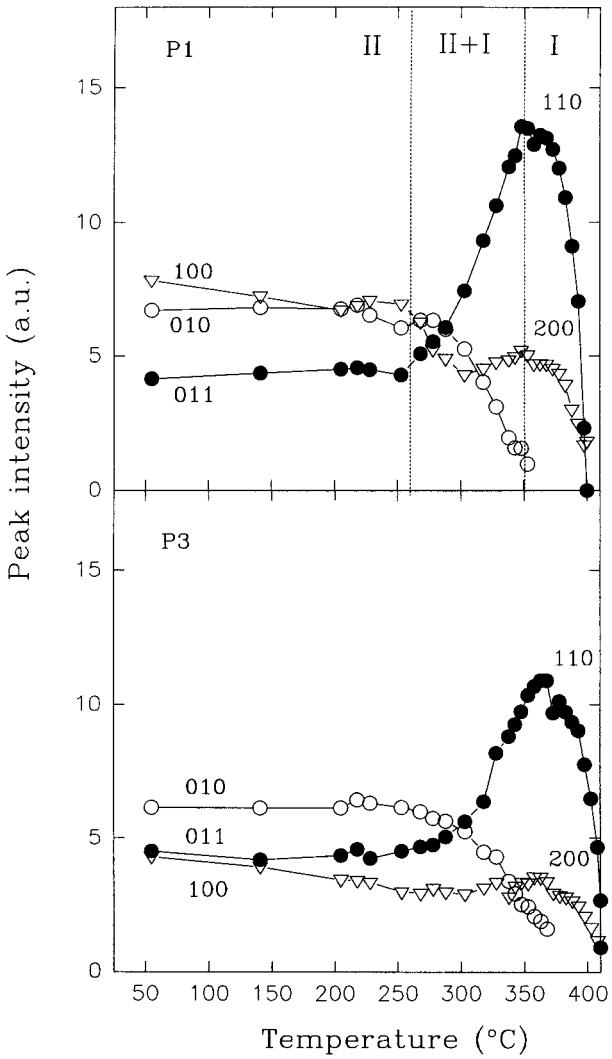

Figure 3. Variation of the peak intensity of the three main reflections of the crystal phase II during its thermal conversion into phase I for samples P1 (top) and P3 (bottom). The phase temperature intervals are indicated by the vertical dot lines.

from linearity, in the 200−300 °C interval, is observed for the 011(II) reflection upon conversion into 110(I). In the case of d_{100} the changes with T are more pronounced and d_{100} shows a broad maximum at about 280−300 °C. This maximum is less broad for the lower molecular weight samples. The maximum in the temperature plot indicates first an increase in expansion coefficient with T and then (above 280 °C) a decrease with T due to the transformation of 100(II) into 200(I). The spacing corresponding to the maximum intensity of the amorphous halo (d_a) is also presented. The d_a temperature plot shows a gradual increase in the expansion coefficient of the disordered material with temperature.

Figure 5 shows the variation of the WAXS crystallinity index (X_c) during heating derived for the three different molecular weight samples. The vertical lines define the temperature intervals of the single phases I and II for P1 and their coexistence region I + II. For P1 there is a slight increase of the index of crystallinity above 200 °C and then it decreases around 260 °C. At higher temperatures X_c goes through a minimum (around 300 °C) and a maximum (around 350 °C) and finally it vanishes due to melting. For P2 better defined minimum and maximum values of X_c than for P1 are observed. For both P1 and P2 samples the X_c value at

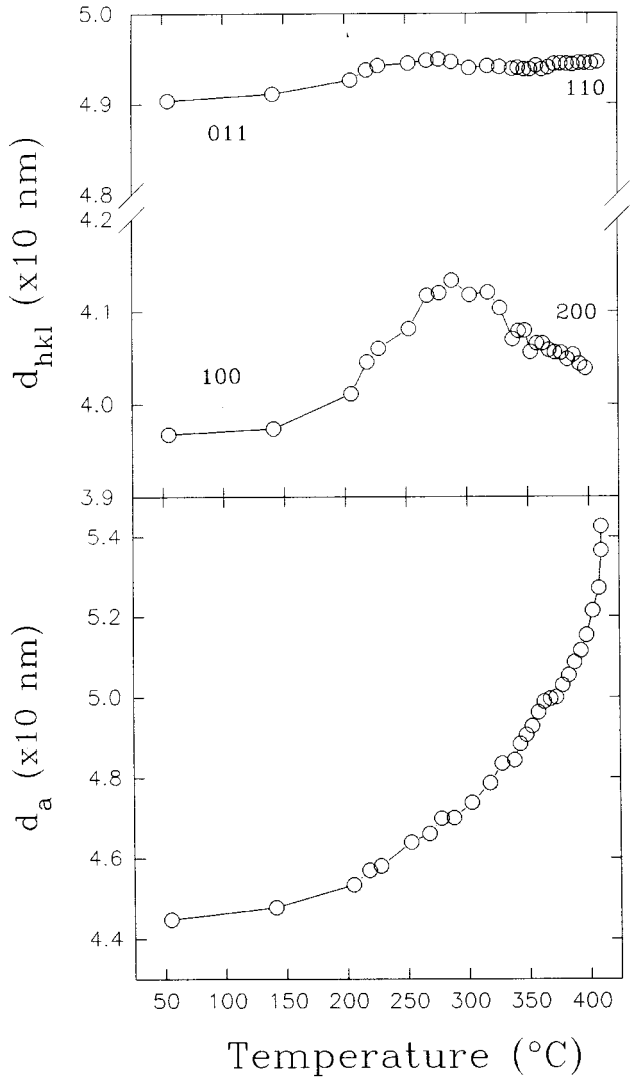

Figure 4. Variation of the lattice spacings of the starting 011-(II) and 100(II) reflections during their conversion into the final 110(I) and 200(I) ones (top) and the spacing calculated from the position of the amorphous halo during heating of sample P3 (bottom).

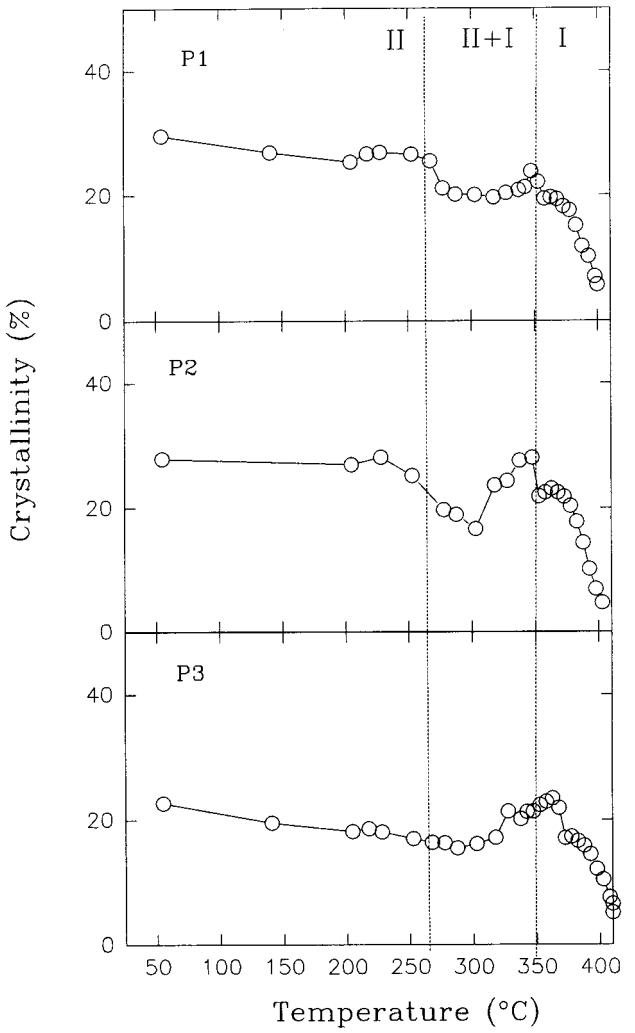

Figure 5. Change of the WAXS crystallinity index observed for the three sintered samples during heating to their melting temperature.

around 350 °C (crystallinity due to phase I exclusively) is similar but not higher than that observed around 200 °C (crystallinity due to phase II). In the case of P3 there is a continuous linear decrease of X_c with temperature up to around 290 °C followed by a maximum at about 360 °C. Now, the X_c value for the maximum (phase I) is clearly larger than that observed in the temperature interval of phase II.

SAXS during a Constant Heating Rate. Figure 2 (bottom) illustrates the SAXS intensity profiles during heating of the samples and the development of the scattering during the first minutes of isothermal crystallization. A strong increase of the scattering intensity is developed upon heating. A weak, broad maximum can be observed, which shifts toward lower angular regions during heating. The corrected SAXS intensity profiles were analyzed by means of a fit program. The long spacing derived from the position of the scattering maxima together with their integrated area is represented in Figure 6 for the three samples. L values increase slightly up to 250 °C and then increase continuously with increasing temperature, as in other polymer systems.[24,25] A close behavior has been reported for PEEK crystallized from the amorphous state.[26,27] Concerning the area of the scattering maxima (total scattered intensity observed), a continuous increase was also observed up to the melting point. After this maximum, the intensity drops abruptly.

Isothermal Crystallization from the Melt. Avrami's Analysis of WAXS Patterns. It is known that aromatic polyketones when crystallized from the molten state show exclusively the more stable crystal phase I. To study the kinetics of an isothermal crystallization process, it is necessary to measure the fraction of crystalline material emerging with time or some other magnitude related to the crystallinity degree. We have selected the maximum intensity of the main 110 reflection of phase I. For that purpose WAXS intensity profiles were resolved into their Gaussian peak components. The Avrami method was then applied to analyze the isothermal crystallization processes by making plots of $\ln(-\ln(1 - I_t/I_{max}))$ vs $\ln(t_c)$.[28] The value I_t refers to the actual 110(I) intensity at the crystallization time t_c, and I_{max}, to the maximum intensity at the end of isothermal crystallization. From the first linear part of the plot we derived the two Avrami parameters: the slope (n) and the ordinate intercept (k). The obtained values are collected in Table 2. The half-crystallization times $t_{1/2}$ calculated according to the formula $t_{1/2} = (\ln 2/k)^{1/n}$ are also presented in Table 2.

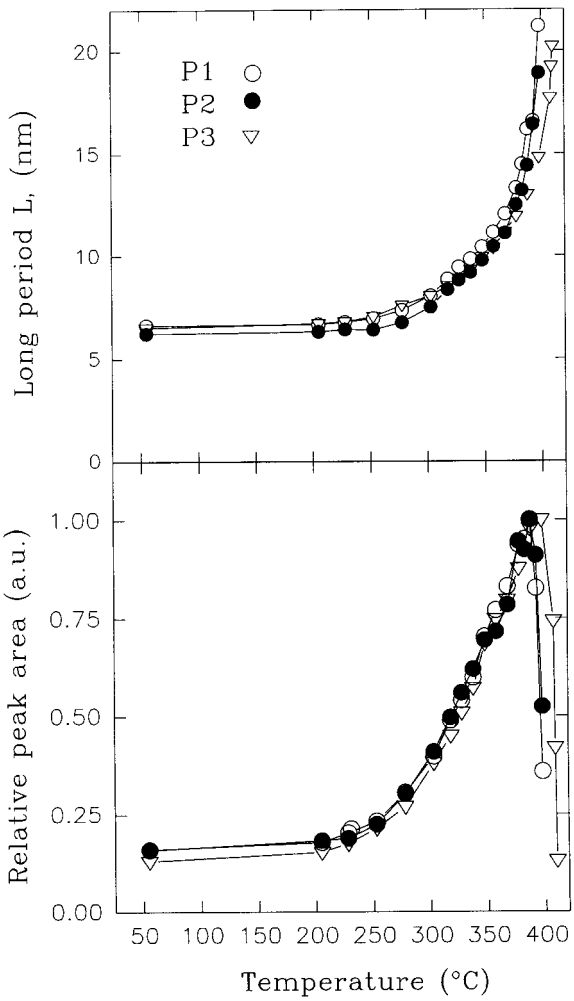

Figure 6. Variation of the long period, L (top), and of the relative intensity of SAXS maxima (bottom) during heating of the samples.

Table 2. Avrami Parameters Calculated from the 110(I) Reflection for Isothermal Melt Crystallized PEKEKK at Different Temperatures, T_c

sample	T_c (°C)	n	k	$t_{1/2}$ (min)
P1	360	0.94	0.109	7.1
	350	1.06	0.131	6.1
P2	343	1.05	0.015	38.3
	333	1.06	0.056	10.5
P3	332	1.10	0.046	11.7
	322	1.02	0.116	5.7

Long Period Development during Melt Crystallization. For all three samples, the SAXS intensity from the molten state is practically negligible (frames recorded at 405 °C that are hidden by the preceding ones in Figure 2 bottom). During the first stages of isothermal crystallization a continuous SAXS profile of rapidly increasing intensity is observed. For longer crystallization times a SAXS maximum becomes resolved.

Lorentz-corrected SAXS intensity profiles show a certain asymmetry from the high scattering angle side, which remains till the end of crystallization and also after cooling the sample to room temperature (Figure 7). The long periodicities were calculated from the angular position of the SAXS maximum. Figure 8 shows the variation observed in the long period during the isothermal crystallization of the samples at the low (filled symbols) and high (open symbols) T_c values investigated. For the shortest crystallization times L decreases rapidly and then levels off. The L values observed at high t_c can be both T_c and molecular weight dependent. Thus, for P1, the two L curves at the two T_c (360 and 350 °C) used are clearly separated from each other and the L values are larger the higher T_c. In the case of P2 and P3, SAXS maxima were only developed for low T_c (333 and 322 °C) values. The L values for P2 are clearly higher than those for P3.

It is noteworthy that the isothermal crystallization experiments at 343 °C for P2 and at 332 °C for P3 yielded the usual development of the WAXS patterns with t_c. However, no SAXS maxima could be simultaneously observed. Indeed, in the case of P2 the SAXS profiles show a continuous scattering during the first 2 h and thereafter incipient SAXS maxima start to appear. For P3 the appearance of incipient SAXS

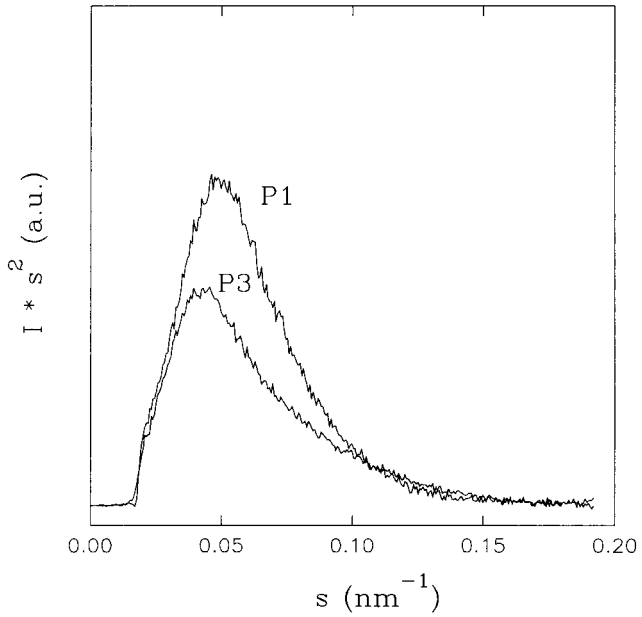

Figure 7. Lorentz-corrected SAXS intensity profiles of samples P1 and P3 after isothermal crystallization at their low T_c for about 3 h.

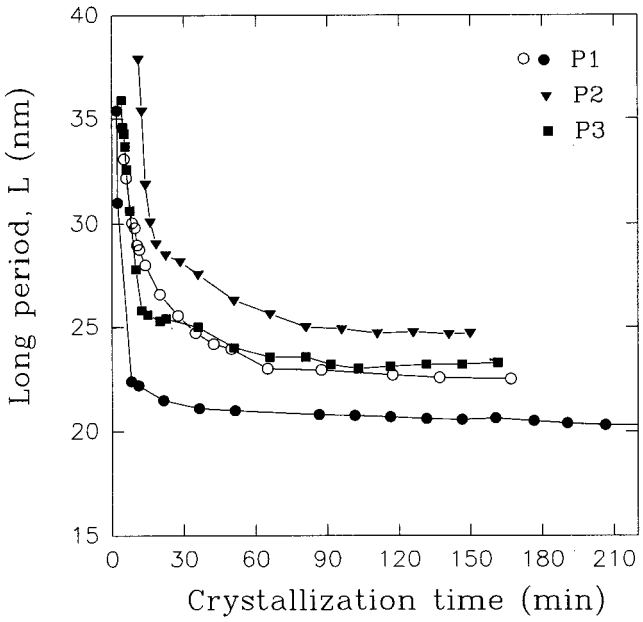

Figure 8. Variation of the long period during the isothermal crystallization time of PEKEKK samples crystallized at the low (filled symbols) and high (open symbols) temperatures T_c.

Table 3. SAXS Peak Asymmetry, Long Period *L* (nm), and Index of Crystallinity X_c (%) Observed after Isothermal Crystallization of PEKEKK Samples at Different Temperatures, T_c[a]

sample	T_c (°C)	SAXS peak asymmetry	L (nm)	X_c (T_c)	X_c (room temp)
P1	360	0.78	22.2	17	41
	350	0.73	20.6	21	–
P2	343	0.80	~29.0	12	30
	333	0.78	24.8	13	35
P3	332	0.63	~30.0	12	18
	322	0.59	23.0	16	34

[a] The index of crystallinity, observed at room temperature, of the isothermal crystallized samples after their cooling is also given.

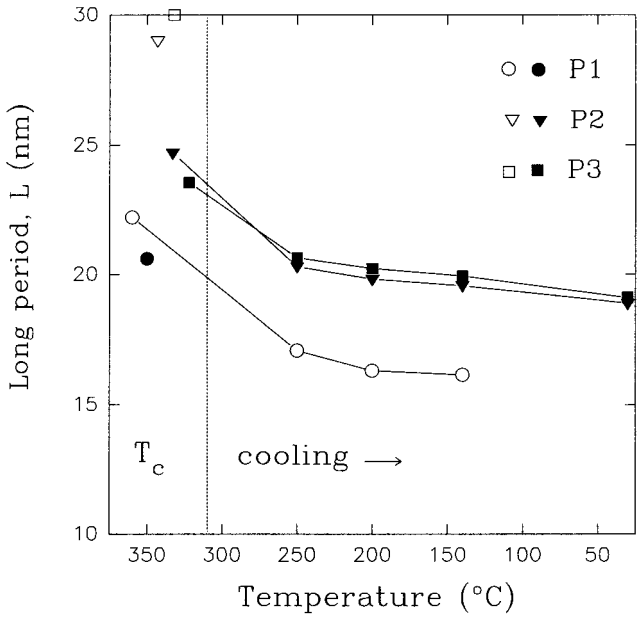

Figure 9. Long period, *L*, obtained for isothermally crystallized polyketones at two different T_c (left) and those observed at different temperatures when one sample of each material is cooled to room temperature (right) (symbols as in Figure 8).

maxima is negligible up to the largest t_c values investigated (3.3 h). Then, the estimated *L* values of P2 and P3 for these particular T_c are about 29−30 nm.

One way to measure the observed asymmetry of SAXS profiles (Figure 7) could be done by calculating the ratio between the half-widths at half-maximum intensity of the left and the right sides of the SAXS profiles. These ratio values, calculated for all the samples for the higest t_c used are collected in Table 3 together with the corresponding *L* values. The asymmetry values are clearly less than 1 (1 means no asymmetry). The P3 sample shows the lowest values, i.e., the largest SAXS peak asymmetry. For each molecular weight sample the lower T_c the higher the asymmetry of the SAXS intensity profiles.

Some of the isothermal crystallization experiments (one for each of the samples) were followed by a cooling in steps toward room temperature. The *L* values observed upon cooling the isothermal crystallized sample down to different temperatures are shown in Figure 9, right side). The *L* values corresponding to isothermally crystallized samples at the high (open symbols) and low (filled ones) T_c values are also represented (left side of Figure 9). On cooling, *L* decreases with decreasing temperature and it levels off for temperatures smaller than 200 °C. The corresponding values of index of crystallinity for each T_c observed for the longest t_c values and those observed at room temperature, after cooling the crystallized samples, are also collected in Table 3.

Discussion

Polymorphism and Phase Transition during Heating. Let us recall that polymorphism of normal aromatic polyketones as revealed by X-ray diffraction is unobserved by DSC, which only shows a single endothermic peak.[20] The discrepancy between the information revealed by both techniques could indicate the isoenthalphic character of the crystal phase transition II to I. Furthermore, the melting temperature depends on the molecular weight and chain defects and also on particle morphology (architecture).[20] The real time WAXS patterns obtained in the present study (Figure 2) confirm the polymorphism observed in aromatic polyketones crystallized in different conditions.[12,13] The results shown in Figures 3 and 4 support the crystal phase transformation of phase II into the more stable phase I during heating of the sample. From these results one may conclude that the phase transition temperature (T_P) at which phase II totally disappears, increases with molecular weight ($T_{P1} \cong 350$ °C; $T_{P2} \cong 357$ °C; $T_{P3} \cong 365$ °C). Taking into account the intensity variation of the 100(II) reflection (Figure 3) and the variation of the crystallinity index X_c shown in Figure 5 one could speak of some time lag in the building up and improvement of the new crystals of phase I in relation to the partial destruction of crystals of phase II upon heating. Furthermore, some influence of the molecular weight on the crystal phase transition cannot be ruled out. Thus, for P1 the X_c values at high temperatures (~350 °C) corresponding to phase I are smaller than those observed for phase II. For the intermediate molecular weight sample (P2) the X_c values are similar for both phases. In the case of P3 the crystallinity observed for phase I is slightly higher than for phase II. Hence, it seems that the crystal phase conversion is partially reduced for the lowest molecular weight sample. The distinct behavior of P3 as compared to P1 or P2 could be also related to the small fraction of material (needle particles) obtained directly in the crystal phase I.[19,20] In the case of P3 the reorganization of material within phase II might be enhanced because of the presence of particles with phase I.

As far as the microstructure is concerned, the results shown in Figure 6 suggest, in addition to its thermal expansion, a continuous reorganization of the material during heating, which is similar for the three samples investigated. Thus both the long periodicities and the scattering intensity increase continuously up to the melting temperature of the samples. This similar SAXS variation, upon heating, of the as-obtained samples could be related to the molecular reorganization inside the isolated particles grown in the reaction medium under similar temperature conditions.[6] From SAXS results, as from DSC calorimetry, there is no evidence of the phase transformation, as detected from WAXS.

Microstructure Development during Isothermal Crystallization from the Melt. The present results indicate that after cooling from the melt, a simultaneous development of SAXS and WAXS takes place. This means that for the time resolution used (less than 1 min), no delay in the appearance of WAXS crystalline

reflections in relation to the SAXS intensity is observed. In other words, in contrast to previous findings on semirigid[21−23] and flexible[29] polymers, no precrystallization phenomena are apparently detected during the melt crystallization of these aromatic polyketones.

For the crystallization temperatures investigated, the PEKEKK samples show no resolved SAXS maximum for the first crystallization times (Figure 8). Furthermore, it is noteworthy that in the case of the higher molecular weight samples (P2 and P3) when crystallized at the high T_c (343 and 332 °C) the appearance of SAXS maxima was considerably delayed (for P2 about 2 h and for P3 after 3 h) in contrast to the early development of typical WAXS patterns. Although the instrumental resolution for the SAXS patterns is not very high (∼40 nm) the absence of L values for the short crystallization times seems rather to indicate an absence of coherence for the electron density fluctuations responsible for discrete SAXS maxima. Therefore, one may expect the emerging crystallizable nuclei to be first randomly distributed (no SAXS maximum) and later, during the initial stages of three-dimensional crystallization, to become correlated and produce the SAXS maximum.

A comparison of the long periods shown in Figures 6 and 8 reveals important aspects of the thermal behavior of these materials:

•The as-obtained material (in particle form) shows L values that are similar for the three investigated samples (Figure 6) and a similar variation of L with increasing temperature up to melting of the samples. The L variation is close to that reported for annealed, amorphous PEEK.[26,27]

•The isothermally melt-crystallized samples show L values that are smaller for the low T_c used (see data of P1 in Figure 8). Furthermore, the relative position of the L curves for the three polyketone samples in Figure 8 would support the influence also of the molecular weight on the microstructure arising under isothermal crystallization.

From the above observations (Figures 6 and 8) and previous results[20] it is apparent that the architecture of the PEKEKK particles plays an important role in the mobility of chains. The particle architecture is presumably destroyed during the thermal treatment before the isothermal crystallization of the samples. As a consequence, the microstructure developed for the isothermally melt-crystallized material becomes more sensitive to the molecular weight and chain regularity. It is known that chain defects would modify the equilibrium melting temperature[30] and would reduce the ability of chains to crystallize in the molten state and during isothermal crystallization. Considering the decreasing T_c values used from P1 to P3 (Table 1) and the increasing variation of L up to a given value of the molecular weight,[18] the microstructure developed by P1 in comparison to those of P2 and P3 (Figure 8) should be mainly controlled by its lower molecular weight. Nevertheless, an additional contribution to the lowering of L values of P1 due to its high chain defect molar content should not be discarded. On the other hand, from the observed L values (Figure 8) the microstructure of P2 and P3 seems to become independent of the molecular weight because of their high viscosity values (high molecular weight, Table 1). Therefore, the L values observed for P2 and P3 should be mainly related to the crystallization temperature used.

The results obtained from isothermally crystallized material after cooling to room temperature (Figure 9 right and Table 3) revealed additional features on the crystallization of aromatic polyketones. The abrupt decrease of L in the interval from T_c to 250 °C could be explained in terms of the insertion model, in which the formation of new thinner crystals between the preexisting ones takes place.[31,32] The further small decrease of L for temperatures below 250 °C may be related to the thermal contraction of the material, similar to the thermal expansion during heating (Figure 4 bottom and Figure 6 top). The low index of crystallinity observed for the isothermally crystallized samples, which is larger for the lower molecular weight sample, increases by a factor of 2.5−2 (P1−P3) after cooling the samples at room temperature (Table 3). It means that additional crystallization of molten material takes place upon cooling.

The close values of the Avrami exponents obtained (see Table 2) suggest a similar crystallization mechanism for the three different molecular weight samples. The k and $t_{1/2}$ experimental values found for the two different T_c show the expected trend; i.e., $t_{1/2}$ increases the larger the T_c for all the investigated samples.[16] Since k and $t_{1/2}$ strongly depend on T_c, it is difficult to compare the samples on the basis of their kinetic parameters (Table 2).

Finally, concerning the above-mentioned asymmetry of SAXS intensity profiles (Figure 7 and Table 3) for each sample it is found that their asymmetry is larger the lower T_c (larger supercooling) is. Furthermore, the largest asymmetry values were observed for the highest molecular weight sample (Table 3). Therefore, it seems that the SAXS peak asymmetry depends on supercooling. In addition, one may think that it could also be dependent on the nature and properties of the molten state. Although the samples were mantained for 10 min in the molten state (25 °C above their melting temperature), still some restriction in chain mobility, because of chain entanglements, may prevent a complete molecular reorganization (ideal molten state). Thus, upon isothermal crystallization together with the preferred interlamellar periodicities developed with t_c, whose sizes (L) are determined by T_c (contribution from more mobile chains), other smaller periodicities would be contributing to the SAXS intensity profiles, producing their asymmetry.

Conclusions

•Upon heating the as-obtained samples, PEKEKK undergoes a polymorphic phase transition (phase II to phase I), as revealed by WAXS.

•A similar, increasing variation of the long period with temperature was observed for the three different molecular weight samples. This is attributed to the similar microstructure developed within the isolated particles grown under similar temperature conditions.

•After destruction of the initial particle morphology through melting, the microstructure arising after isothermal crystallization is very much dependent on the crystallization temperature (supercooling). For the lowest viscosity sample (P1) the microstructure is also dependent on molecular weight while for the higher viscosity samples (P2 and P3) are not molecular weight dependent.

•The Avrami analysis of WAXS patterns reveals a similar crystallization mechanism for the three molec-

ular weight samples isothermally crystallized from the melt.

Acknowledgment. The authors acknowledge the facilities found at the Polymer beamline A2 of HASYLAB, DESY, Hamburg, and the funding from the Program Human Capital and Mobility, Access to Large Installations EC. Grateful acknowledgment is due to DGICYT, Spain (grant PB94/0049), and to NEDO's International Joint Research Program, Japan, for the generous support of this investigation.

References and Notes

(1) Staniland, P. A. In *Comprehensive Polymer Science*; Allen, G., Bevington, J. C., Eds.; Pergamon: Oxford, U.K., 1989; Vol. 5, pp 483−497.
(2) Mullins, M. J.; Woo, E. P. *J. Macromol. Sci., Rev. Macromol. Chem. Phys.* **1987**, *C27*, 313.
(3) *Handbook of polymer synthesis*; Kricheldorf, H. R., Ed.; Marcel Dekker: New York, 1992; Part A; p 545.
(4) Zolotukhin, M. G.; Gileva, N. G.; Sedova, E. A.; Egorov, A. E.; Sangalov, Yu. A.; Salazkin, S. N.; Lebedev, Yu. A. *Dokl. Akad. Nauk SSSR* **1989**, *304*, 378.
(5) Gileva, N. G.; Zolotukhin, M. G.; Salazkin, S. N.; Sultanova, V. S.; Hörhold, H. H.; Raabe, D. *Acta Polym.* **1988**, *39*, 452.
(6) Zolotukhin, M. G.; Rueda, D. R.; Baltá Calleja, F. J.; Bruix, M.; Cagiao, M. E.; Bulai, A.; Gileva, N. G. *Macromol. Chem. Phys.* **1997**, *198*, 1131.
(7) Boom, J.; Magre, E. P. *Makromol. Chem.* **1969**, *126*, 130.
(8) Dawson, P. C.; Blundell, D. J. *Polymer* **1980**, *21*, 577.
(9) Rueda, D. R.; Ania, F.; Richarson, A.; Ward, I. M.; Baltá-Calleja, F. J. *Polym. Commun.* **1983**, *24*, 258.
(10) Wakelyn, N. T. *Polym. Commun.* **1984**, *25*, 306.
(11) Blundell, D. J.; Newton, A. B. *Polymer* **1991**, *32*, 308.
(12) Gardner, K. H.; Hsiao, B. S.; Matheson, R. R., Jr.; Wood, B. A. *Polymer* **1992**, *33*, 2483.
(13) Gardner, K. H.; Hsiao, B. S.; Faron, K. L. *Polymer* **1994**, *35*, 2290.
(14) Day, M.; Deslandes, Y.; Roovers, J.; Suprunchuk, T. *Polymer* **1991**, *32* (7), 1258.
(15) Xin Lu, S.; Cebe, P.; Capel, M. *Macromolecules* **1997**, *30*, 6243.
(16) Lovinger, A. J.; Davis, D. D.; Padden, F. J., Jr. *Polymer* **1985**, *26*, 1595.
(17) López, L. C.; Wilkes, G. L. *Polymer* **1988**, *29*, 106.
(18) Rault, J. *CRC Crit. Rev. Solid State Mater. Sci.* **1986**, *13*, 57.
(19) Zolotukhin, M. G.; Baltá Calleja, F. J.; Rueda, D. R.; Palacios, J. M. *Acta Polym.* **1997**, *48*, 269.
(20) Rueda, D. R.; Zolotukhin, D. R.; Cagiao, M. E.; Baltá Calleja, F. J.; Villers, D.; Dosière, M. *Macromolecules* **1996**, *29* (22), 7016.
(21) Imai, M.; Kaji, K.; Kanaya, T. *Phys. Rev. Lett.* **1993**, *71*, 4162.
(22) Imai, M.; mori, K.; Mizukami, T.; Kaji, K.; Kanaya, T. *Polymer* **1992**, *33*, 4451.
(23) Ezquerra, T. A.; López-Cabarcos, E.; Hsiao, B. S.; Baltá Calleja, F. J. *Phys. Rev. E* **1996**, *54*, 989.
(24) Fischer, E. W.; Schmidt, G. F. *Angw. Chem.* **1962**, *74*, 551.
(25) Fakirov, S.; Fischer, E. W.; Schmidt, G. F. *Makromol. Chem.* **1979**, *176*, 2459.
(26) Lee, Y.; Porter, R. S.; Lin, J. S. *Macromolecules* **1989**, *22*, 1756.
(27) Fougnies, C.; Damman, P.; Dosière, M.; Koch, M. H. J. *Macromolecules* **1997**, *30*, 1385.
(28) Wunderlich, B. *Macromolecular Physics: 2. Crystal Nucleation Growth, Annealing*; Academic Press: New York, London, 1978.
(29) Hsiao, B. S.; Nogales, A.; Ezquerra, T. A.; Baltá Calleja, F. J.; Sauer, B. B.; Seifert, S.; Kaparu, Y.; Stein, R.; Muthukuman, M.; Koch, M. *Bull. Am. Phys. Soc.* **1997**, *42* (1), 585.
(30) Wunderlich, B. *Macromolecular Physics: 3. Crystal Melting*; Academic Press: New York, London, 1980.
(31) Hsiao, B. S.; Gardner, K. H.; Wu. D. Q.; Chu, B. *Polymer* **1993**, *34*, 3986.
(32) Krüger, K. N.; Zachmann, H. G. *Macromolecules* **1993**, *26*, 5202.

MA980440Z